

## Second ballooning stability in high- $\beta$ , compact stellarators<sup>a)</sup>

A. S. Ware,<sup>1,b)</sup> D. Westerly,<sup>1</sup> E. Barcikowski,<sup>1</sup> L. A. Berry,<sup>2</sup> G. Y. Fu,<sup>3</sup> S. P. Hirshman,<sup>2</sup> J. F. Lyon,<sup>2</sup> R. Sanchez,<sup>4</sup> D. A. Spong,<sup>2</sup> and D. J. Strickler<sup>2</sup>

<sup>1</sup>University of Montana, Missoula, Montana 59812

<sup>2</sup>Oak Ridge National Laboratory, Oak Ridge, Tennessee 37831

<sup>3</sup>Princeton Plasma Physics Laboratory, Princeton, New Jersey 08543

<sup>4</sup>Universidad Carlos III de Madrid, Madrid, Spain

(Received 31 October 2003; accepted 23 December 2003; published online 23 April 2004)

Second ballooning stability is examined in quasipoloidally symmetric, compact stellarator configurations. These high- $\beta$  (volume-average  $\beta > 4\%$ ) free-boundary equilibria are calculated using a reference Quasi-Poloidal Stellarator (QPS) configuration. QPS plasmas have low-shear, stellarator-like rotational transform profile with  $|B|$  that is approximately poloidally symmetric. The high- $\beta$  QPS equilibria are similar in their magnetic configuration to previously studied tokamak-stellarator hybrids which have a high-shear, tokamak-like rotational transform profile. Both types of configurations have strong magnetic wells and consequently high interchange stability  $\beta$  limits. Free-boundary QPS equilibria have regions of second stability at high  $\beta$ . For infinite- $n$  ballooning modes in QPS plasmas, the boundary for first instability is  $\langle\beta\rangle \sim 2\%$  and the boundary for second stability is  $\langle\beta\rangle \sim 6\%$ . Finite- $n$  ballooning mode calculations show higher  $\beta$  limits,  $\langle\beta\rangle > 5\%$ . Increasing plasma current (for fixed plasma pressure) can lower the finite- $n$  ballooning mode  $\beta$  limit to  $\langle\beta\rangle = 3\%$  by reducing magnetic shear. QPS plasmas with Ohmic current profiles (peaked on-axis) have both a lower infinite- $n$  ballooning  $\beta$ -limit for the onset of first instability and a higher  $\beta$ -limit for the onset of second stability relative to QPS plasma with bootstrap current profiles (peaked off-axis). QPS plasmas are stable to low- $n$  ideal magnetohydrodynamic kink modes and vertical modes for values of  $\beta$  in this range ( $\langle\beta\rangle \sim 6\%$ ) due to the low level of plasma current in QPS relative to an equivalent tokamak. © 2004 American Institute of Physics. [DOI: 10.1063/1.1651101]

### I. INTRODUCTION

High-energy density, compactness, and steady-state operation are all attractive features for a fusion reactor. Stability limits of ideal magnetohydrodynamic (MHD) interchange modes may limit the obtainable  $\beta$  in three-dimensional magnetic configurations, thus limiting the achievable energy-density (though to date there is no experimental evidence of a  $\beta$ -limit due to local interchange modes in a stellarator). Here,  $\beta$  is the ratio of the plasma pressure to the magnetic pressure,  $\beta = p/B^2$ , and  $\langle\beta\rangle$  indicates the volume average  $\beta$ .

The designs of a number of recent stellarator experiments have incorporated quasisymmetry in the magnetic spectrum in order to achieve improved neoclassical confinement.<sup>1–3</sup> The improved confinement has allowed the design of compact stellarator experiments. Among these quasisymmetric configurations, the most compact stellarator design is that of the Quasi-Poloidal Stellarator (QPS, a proposed quasipoloidally symmetric device).<sup>3,4</sup> Quasipoloidal symmetry is defined as the magnetic field strength,  $|B|$ , being independent of the poloidal angle,  $\partial B/\partial\theta \approx 0$ , in flux coordinates. QPS is a two-field period device with a racetrack shape and very small aspect ratio,  $A < 3$ , where  $A$  is the ratio of the average major radius to the average minor radius. A reference QPS configuration is described in the next section. The focus of this work is the stability properties of QPS

plasma at high- $\beta$ . While the planned experimental program for QPS calls for operation up to  $\langle\beta\rangle = 3\% - 4\%$ , similarities in the magnetic spectrum between QPS and a class of tokamak-stellarator hybrid configurations which have very-high MHD stability  $\beta$  limits<sup>5</sup> has led us to examine the properties of high- $\beta$  QPS plasma. Here, high- $\beta$  in QPS refers to plasmas in the range  $\langle\beta\rangle = 4\% - 8\%$ . In particular, second-stability access in the QPS configuration is explored.

Second ballooning stability is a region of interchange stability for large pressure gradients.<sup>6</sup> Access to second ballooning stability in axisymmetric devices makes possible advanced tokamak operation at high- $\beta$ . There has been some concern expressed that a region of second stability does not exist in stellarator plasmas<sup>7</sup> due to an unavoidable overlap of regions of bad curvature and weak shear in three-dimensional geometry. More recent work, however, indicates that a second stability does exist for some stellarator configurations at very large pressure gradients.<sup>5,8</sup> Previous numerical investigations into second stability in stellarator configurations have been restricted to fixed-boundary equilibria. That is, the effect of high- $\beta$  on the shape of the outer plasma boundary was neglected. In this work, we present numerical calculations of free-boundary plasmas using a reference QPS coil set that exhibit regions of second ballooning stability. In addition, we show that plasma current and plasma current profile impact ballooning stability.

This paper is organized as follows: In Sec. II, the QPS coil configuration and equilibrium properties are described.

<sup>a)</sup>Paper LI1 4, Bull. Am. Phys. Soc. **48**, 199 (2003).

<sup>b)</sup>Invited speaker. Electronic mail: aware@selway.umt.edu

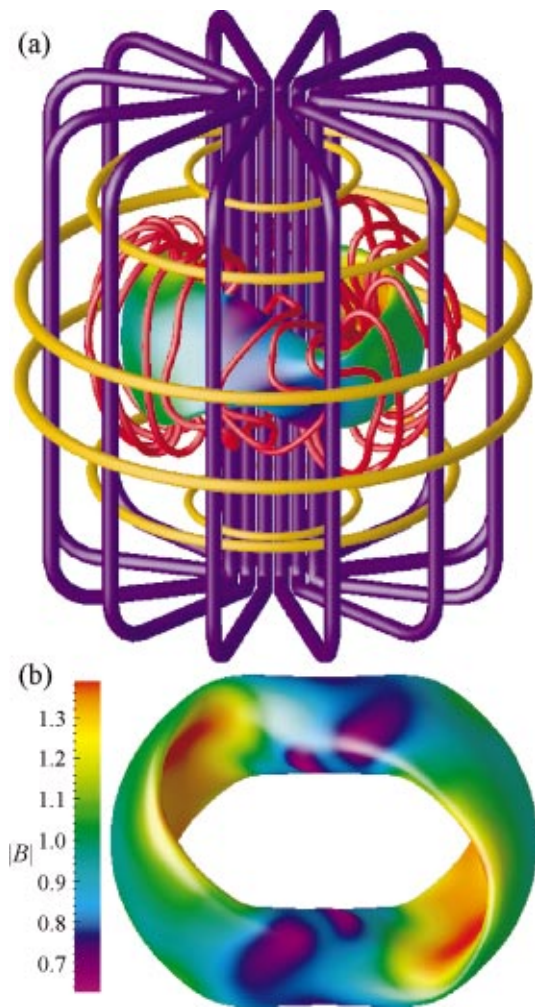


FIG. 1. (Color) (a) Reference QPS coil set (modular coils in red, vertical field coils in yellow, and toroidal field coils in blue) with the last-closed-flux surface and (b) an overhead view of the last-closed-flux surface, color on the surface indicating  $|B|$ .

Section III describes the region of second ballooning stability in QPS plasma. The impact of plasma current on ballooning stability is discussed in Sec. IV. Stability calculations for low- $n$  modes are presented in Sec. V. Finally, some discussion and conclusions are contained in Sec. VI.

## II. THE QPS CONFIGURATION

The coils and outer plasma surface for a reference QPS configuration are shown in Fig. 1. The coil set includes 20 modular coils with 5 distinct coil types, 3 pairs of circular vertical field coils, and 12 toroidal field coils. More details on the coils and the process used to optimize the QPS coil configuration can be found in Ref. 4. The 3D equilibrium code VMEC (Ref. 9) is used to obtain the finite- $\beta$  equilibria. The reference configuration has 300 kA of current in the modular coils, -129, -76, and 0 kA in the small, medium, and large vertical field coils, and -25 kA in the toroidal field coils. The design of the QPS experiment incorporated a current profile fully compatible (“aligned”) with the bootstrap current. The VMEC equilibrium current, the pressure profile, and the rotational transform profile for the reference configuration are shown in Fig. 2. The pressure profile used to test stability is a simple quadratic profile,  $p = p_0(1 - S)^2$ , where  $S$  is the normalized toroidal flux [ $S \sim (r/a)^2$ ]. The reference configuration has 11 kA of net parallel bootstrap current at  $\langle \beta \rangle = 2\%$ . This value of bootstrap current is 1/4 the full collisionless bootstrap current and is appropriate for the more collisional operating regime expected in QPS. In the following, when testing stability at higher  $\beta$ , the bootstrap current is scaled proportionately with  $\langle \beta \rangle$  (e.g., 22 kA of current at  $\langle \beta \rangle = 4\%$ ).

The impact of increasing  $\langle \beta \rangle$  and the Shafranov shift in QPS is shown in Fig. 3 which contains cross sections of flux surfaces at the bean-shaped cross section. As  $\langle \beta \rangle$  is increased

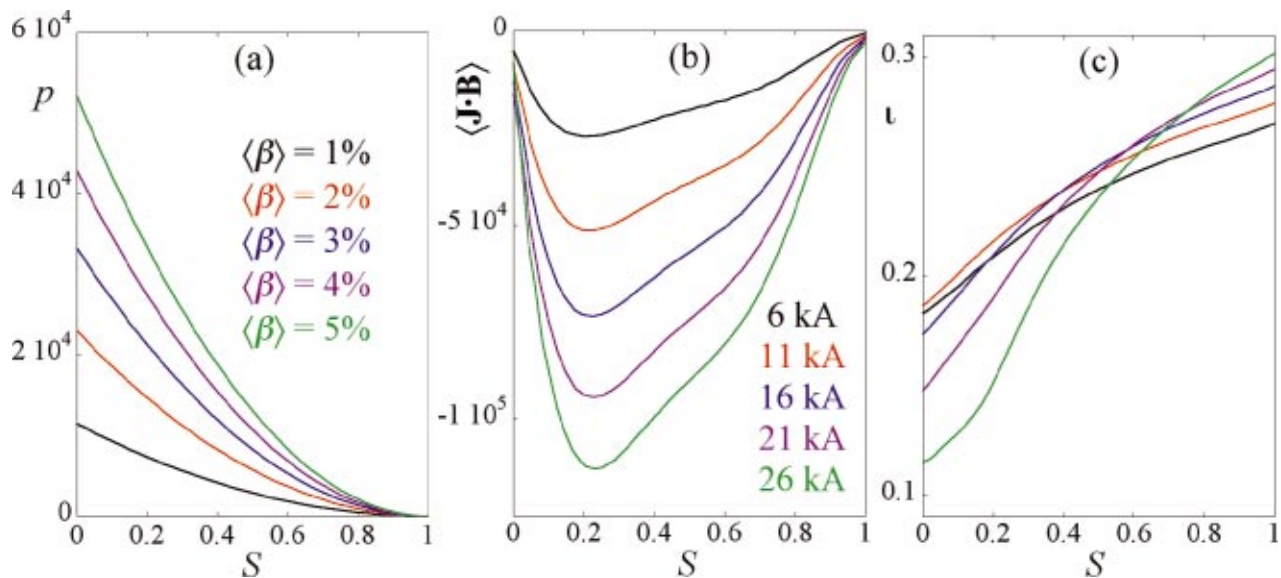


FIG. 2. (Color) Profiles of (a) pressure, (b) field-aligned current, and (c) rotational transform for  $\langle \beta \rangle = 1\%, 2\%, 3\%, 4\%$ , and  $5\%$  with plasma current 6, 11, 16, 21, and 26 kA, respectively.

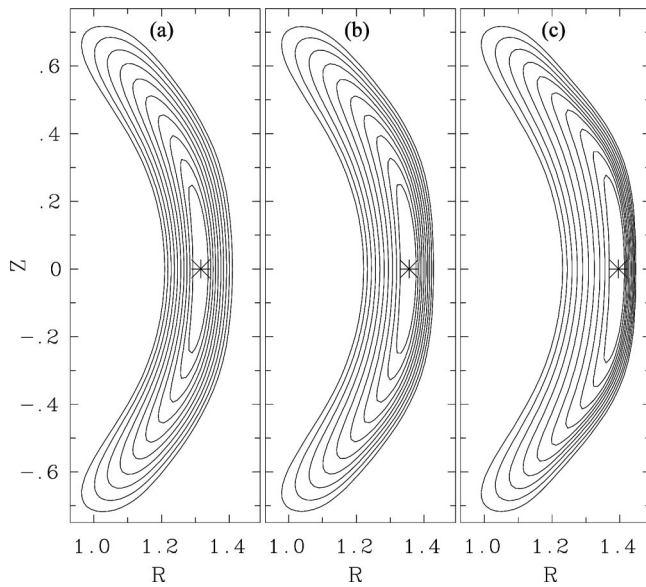


FIG. 3. Cross sections of magnetic flux surfaces at the bean-shaped cross section for three of the cases shown in Fig. 2: (a)  $\langle\beta\rangle=1\%$  with 6 kA of plasma current, (b)  $\langle\beta\rangle=3\%$  with 16 kA of plasma current, and (c)  $\langle\beta\rangle=5\%$  with 26 kA of plasma current.

from 1% to 5%, the magnetic axis shifts outward to a greater degree than the outer surface. The flux surfaces become compressed towards the outside of the torus and this effect is strongest in the bean-shaped cross section. This Shafranov shift is a by-product of the low aspect ratio of QPS. In other words, the dominant symmetry breaking term is the toroidal curvature term (an  $n=0$ ,  $m=1$  component in the magnetic spectrum). The degree of quasipoloidal symmetry in QPS is limited by the constraint of low aspect ratio.<sup>10</sup> This does not imply that the degree of quasipoloidal symmetry decreases with increasing  $\beta$ . Indeed, the opposite is true in that the degree of quasi-poloidal symmetry increases weakly with  $\beta$ .

The plasma shape can be modified using the vertical field coils. The effect of increasing currents in the vertical field coils is shown in Fig. 4. The cross sections at two different toroidal angles from QPS plasmas with  $\langle\beta\rangle=7\%$  are shown in Figs. 4(a) and 4(b) with the cross sections in black for  $-128$ ,  $-75$ , and  $0$  kA in the small, medium, and large vertical field coils, respectively, and the cross sections in red for  $-257$ ,  $-150$ , and  $-50$  kA in the small, medium, and large vertical field coils, respectively. In Figs. 4(c) and 4(d), the same cross sections are shown with the magnetic axes shifted so that they overlap for the two cases. It is clear from these figures that the increase in vertical field has not significantly reduced the compression of flux surfaces at high- $\beta$ .

The QPS device will have the capability of operating with Ohmic current. Figure 5(a) shows three different field-aligned current profiles for QPS. These consist of a bootstrap profile optimized to match the predicted bootstrap current, an Ohmic profile peaked on axis, and a hybrid profile corresponding to an average of the other profiles. The corresponding rotational transform profiles for a QPS plasma with  $\langle\beta\rangle=2\%$  and a total plasma current of 41 kA are shown in Fig. 5(b). The Ohmic current results in a reverse-shear rotational transform profile even for this small amount of cur-

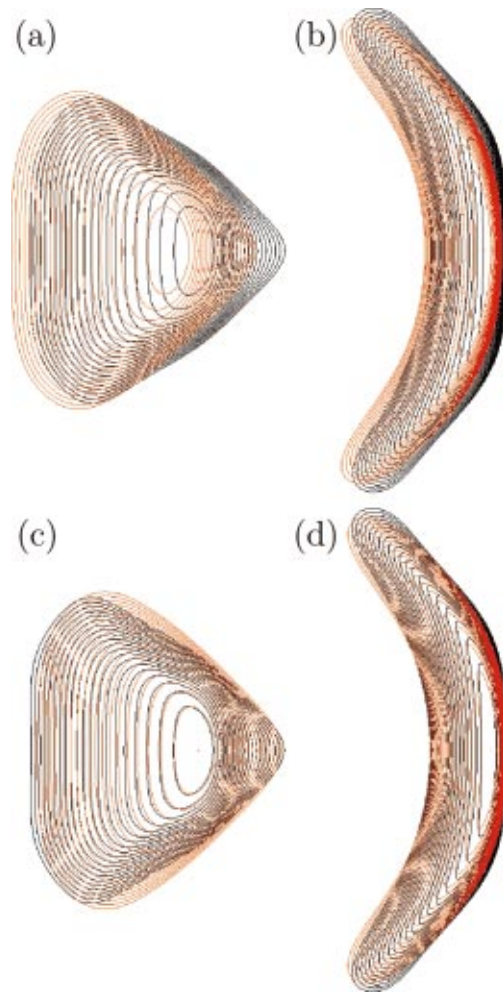


FIG. 4. (Color) Cross sections of magnetic flux surfaces at the (a) bean-shaped and (b) triangular cross sections for an equilibrium with  $\langle\beta\rangle=7\%$  with 52 kA of plasma current. In black are the cross sections for currents of  $-128$ ,  $-75$ , and  $0$  kA in the small, medium, and large vertical field coils while in red are the cross sections with these currents increased to  $-257$ ,  $-150$ , and  $-50$  kA, respectively. The same cross sections are shown in (c) and (d) with the axes shifted so that the magnetic axes overlap.

rent. The impact of the different current profiles on ballooning stability is discussed in Sec. IV.

### III. SECOND BALLOONING STABILITY IN QPS

The VMEC code is used to obtain an equilibrium and infinite- $n$  ballooning mode stability is analyzed using the COBRAVMEC stability code.<sup>11</sup> COBRAVMEC solves for the most unstable ballooning mode on a given surface using Richardson extrapolation to VMEC coordinates without the need for a transformation to Boozer coordinates. For the reference configuration, a quadratic pressure profile,  $p(S)=p_0(1-S)^2$ , was chosen for simplicity. Ballooning growth rates as a function of the normalized flux,  $S$ , are shown in Fig. 6(a). As the plasma pressure is increased, the plasma first becomes ballooning unstable at  $\langle\beta\rangle\approx 2\%$ . The region of instability grows until  $\langle\beta\rangle\approx 6\%$ , where a region of second stability appears as shown in Fig. 6(b). Optimization for stability via variation of

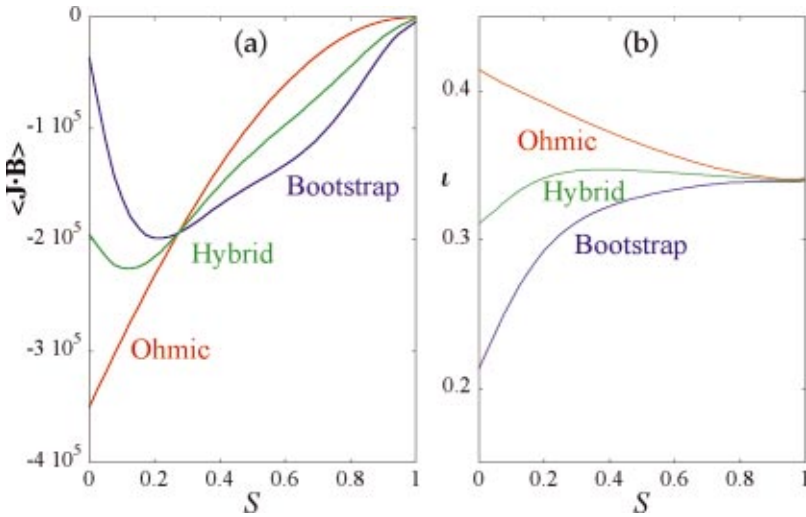


FIG. 5. (Color) (a) Three field-aligned current profiles used to test the impact of the plasma current profile on access to second stability and (b) the respective rotational transform profiles for these current profiles.

the plasma current profile, pressure profiles, and the currents in the external coils can minimize the gap between first and second stability to  $\langle \beta \rangle = 2.5\% - 5.5\%$ .

All of the infinite- $n$  ballooning stability results shown in Fig. 6 and throughout the remainder of this paper have been calculated using  $\theta_k = 0$  and  $\alpha = 0$ . Here,  $\theta_k$  is the ballooning parameter and is equivalent to the ratio of radial to toroidal wave numbers, while  $\alpha$  is a field line label.<sup>12</sup> Calculations using the COBRAVMEC code indicate these values of  $\theta_k$  and  $\alpha$  correspond to the first field line to go unstable as  $\beta$  is increased (i.e., they determine the boundary for first instability). However, while all values of  $\theta_k$  and  $\alpha$  tested showed signs of second stability at high- $\beta$ , a systematic study of the sensitivity of the boundary for second stability on these parameters has not been undertaken. The actual boundary for second stability is likely at higher- $\beta$  than shown here.

#### IV. IMPACT OF THE PLASMA CURRENT PROFILE ON BALLOONING STABILITY

In addition to the total plasma current, the plasma current profile can also impact ballooning stability. As shown earlier in Fig. 5, going from a bootstrap current profile to an

Ohmic current profile in QPS reverses the sign of the shear. Equilibria were obtained for a range of  $\langle \beta \rangle$  at a fixed plasma current of 41 kA.

The ballooning stability results from COBRAVMEC are shown in Fig. 7 as contour plots of the growth rate versus normalized flux,  $S$ , and  $\langle \beta \rangle$ . The gap between first and second stability is largest for the Ohmic current profile and smallest for the bootstrap current profile. For the bootstrap current profile, the plasma becomes unstable at  $\langle \beta \rangle > 2\%$  and exhibits regions of second stability for  $\langle \beta \rangle > 5.5\%$ .

The COBRAVMEC code calculates the local (on a field line) ballooning growth rate in the infinite- $n$  limit. The stability of QPS plasma to finite- $n$  ballooning modes is examined using the global MHD stability code TERPSICHORE.<sup>13</sup> Ballooning mode eigenvalues ( $\propto \omega^2$ ) from TERPSICHORE are shown in Fig. 8 for a number of QPS cases. Negative eigenvalues indicate unstable modes. With the plasma current scaled with  $\langle \beta \rangle$  as shown in Fig. 2, QPS is stable to finite- $n$  (up to  $n = 19$ ) ballooning modes for  $\langle \beta \rangle > 5\%$ . If the plasma current is doubled (as might be expected for a less-collisional plasma), QPS becomes unstable to a finite- $n$  ballooning mode for  $\langle \beta \rangle > 3\%$ .

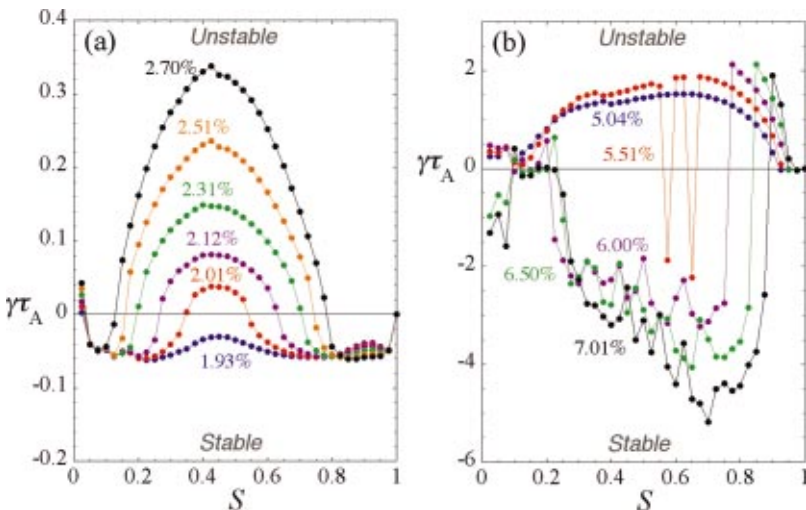


FIG. 6. (Color) Ballooning growth rates from COBRAVMEC as a function of the normalized flux,  $S$ , for various  $\langle \beta \rangle$ , indicating (a) the first stability boundary and (b) the onset of second stability.

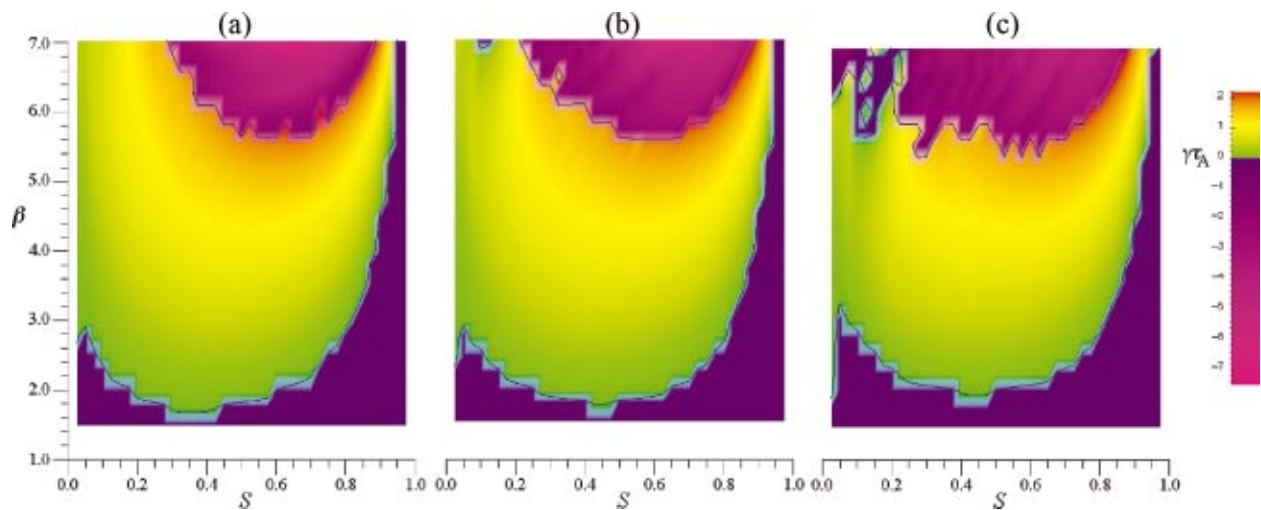


FIG. 7. (Color) Contour plots of the ballooning growth rates from COBRAVMEC as a function of  $S$  and  $\langle\beta\rangle$  for the three different current profiles shown in Fig. 5: (a) Ohmic, (b) hybrid, and (c) bootstrap.

## V. LOW- $n$ MHD STABILITY OF QPS AT HIGH- $\beta$

The finite plasma current in these configurations makes them potentially susceptible to vertical and kink modes. The stability of QPS plasma to kink and vertical modes is also analyzed using the TERPSICHORE code. There are two families of low- $n$  modes in a two-field period device: an  $n=0$  family and an  $n=1$  family. The  $n=0$  family is classified as a vertical mode and couples together even toroidal mode numbers while the  $n=1$  family is classified as a kink mode and couples together odd toroidal mode numbers. In spite of the finite plasma current and high- $\beta$ , QPS plasmas are stable to kink and vertical modes for  $\langle\beta\rangle > 5\%$ . In contrast to finite- $n$  ballooning modes, increased plasma current results in QPS plasmas being stable at higher  $\beta$  ( $\langle\beta\rangle > 6\%$ ). Work is underway to test the impact of increased Ohmic current on low- $n$  mode stability.

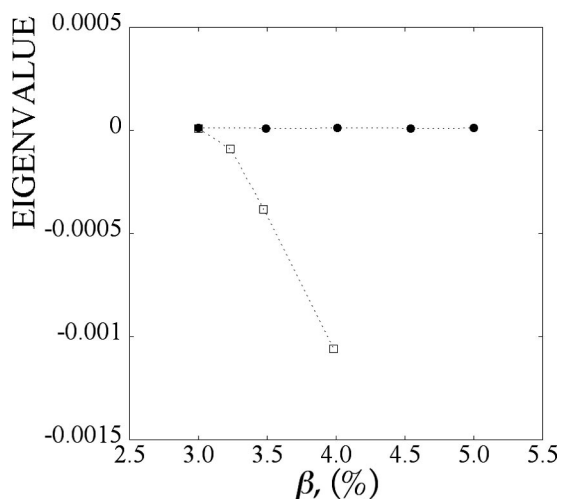


FIG. 8. Finite- $n$  ballooning mode eigenvalues from TERPSICHORE as a function of  $\langle\beta\rangle$  for scans with the base level of bootstrap current (closed circles) and with twice the base level of bootstrap current (open squares).

## VI. CONCLUSIONS

A region of second ballooning stability has been shown for free-boundary, three-dimensional plasma equilibria. In QPS plasmas, a large region of the plasma becomes second stable for  $\langle\beta\rangle \sim 6\%$ . The plasma current profile impacts the gap between first and second stability with a bootstrap current profile resulting in the smallest gap. The total plasma current also impacts the finite- $n$  ballooning stability of QPS plasmas. Increased plasma current results in decreased magnetic shear and a reduced  $\beta$ -limit for stability to finite- $n$  ballooning modes.

The implications for the possibility of operating QPS at high- $\beta$  are mixed. While further optimizations may reduce the gap between first and second stability boundaries, the infinite- $n$  ballooning results presented here would seem to limit high- $\beta$  operation in QPS. However, finite- $n$  ballooning results show higher- $\beta$  plasmas with modest bootstrap current in QPS are ballooning stable. Also, as previously mentioned, no stellarator experiment has documented a  $\beta$ -limit due to local interchange modes. This may imply that nonideal effects such as finite Larmor radius limit the degradation due to infinite- $n$  ballooning modes.

## ACKNOWLEDGMENTS

This research was supported by the U.S. DOE under Grant No. DE-FG 02-03ER54699 at the University of Montana and under Contract No. DE-AC05-00OR22725 at Oak Ridge National Laboratory, managed by UT-Battelle, LLC. Some of the calculations presented were performed using the facilities at the National Energy Research Scientific Computing Center.

<sup>1</sup>D. T. Anderson, A. Almagri, F. S. B. Anderson *et al.*, J. Plasma Fusion Res. **1**, 49 (1998).

<sup>2</sup>G. H. Neilson, A. H. Reiman, M. C. Zarnstorff *et al.*, Phys. Plasmas **7**, 1911 (2000).

<sup>3</sup>J. F. Lyon, L. A. Berry, M. C. Cole *et al.*, "Physics and engineering design

of a very-low-aspect-ratio quasi-poloidal stellarator," Nucl. Fusion (in preparation).

- <sup>4</sup>D. J. Strickler, S. P. Hirshman, D. A. Spong, M. J. Cole, J. F. Lyon, B. E. Nelson, D. E. Williamson, and A. S. Ware, *Fusion Sci. Technol.* **45**, 15 (2004).
- <sup>5</sup>A. S. Ware, S. P. Hirshman, D. A. Spong, L. A. Berry, A. J. Deisher, G. Y. Fu, J. F. Lyon, and R. Sanchez, *Phys. Rev. Lett.* **89**, 125003 (2002).
- <sup>6</sup>R. D. Hazeltine and J. D. Meiss, *Plasma Confinement* (Addison-Wesley, Redwood City, 1992), pp. 309–312.
- <sup>7</sup>C. C. Hegna and S. R. Hudson, *Phys. Plasmas* **9**, 2014 (2002).
- <sup>8</sup>S. R. Hudson and C. C. Hegna, *Phys. Plasmas* **10**, 4716 (2003).
- <sup>9</sup>S. P. Hirshman and J. C. Whitson, *Phys. Fluids* **26**, 3553 (1983).
- <sup>10</sup>D. A. Spong, D. J. Strickler, S. P. Hirshman, J. F. Lyon, L. A. Berry, D. Mikkelsen, D. Monticello, and A. S. Ware, "QPS transport physics flexibility using variable coil currents," *Fusion Sci. Technol.* (submitted).
- <sup>11</sup>R. Sanchez, S. P. Hirshman, and V. Wong, *Comput. Phys. Commun.* **135**, 82 (2001).
- <sup>12</sup>R. L. Dewar and A. H. Glasser, *Phys. Fluids* **26**, 3038 (1983).
- <sup>13</sup>W. A. Cooper, D. B. Singleton, and R. L. Dewar, *Phys. Plasmas* **3**, 275 (1996).